Frequency-domain Iterative MUI Cancellation for Uplink SC-FDMA Using Frequency-domain Filtering

Suguru OKUYAMA† Kazuki TAKEDA† and Fumiyuki ADACHI‡
Dept. of Electrical and Communication Engineering, Graduate School of Engineering, Tohoku University
6-6-05 Aza-Aoba, Aramaki, Aoba-ku, Sendai, 980-8579 Japan
E-mail: †{okuyama, kazuki}@mobile.ecei.tohoku.ac.jp, ‡adachi@ecei.tohoku.ac.jp

***Abstract*—The peak-to-average power ratio (PAPR) of Nyquist filtered broadband single carrier (SC)-FDMA signals can be reduced by increasing the filter roll-off factor α. Furthermore, an additional frequency diversity gain can be obtained by making use of the excess bandwidth introduced by the transmit filtering. However, if the carrier-frequency separation is kept the same as in the case of α=0, the adjacent users' signal spectra overlap with the desired users' spectrum and the multiuser interference (MUI) is produced. In this paper, in order to improve the transmission performance of uplink SC-FDMA using frequency-domain filtering, we propose two type of frequency-domain iterative MUI cancellation scheme which can achieve the frequency diversity gain through MMSE-FDE&spectrum combining. The achievable bit error rate (BER) and throughput performances are evaluated by computer simulation.**

Keywords-component; SC-FDMA, MUI cancellation, frequency-domain filtering

I. INTRODUCTION

For the next generation mobile communication systems, high-speed and high-quality data services are demanded. Since the broadband wireless channel is composed of many propagation paths having different time delays, the bit error rate (BER) performance degrades due to inter-symbol interference (ISI) arising from frequency-selective fading channel [1],[2]. Orthogonal frequency division multiplexing (OFDM) converts the frequency-selective channel into a number of orthogonal frequency-nonselective channels (sub-carriers) and alleviates the ISI problem [3],[4]. However, OFDM has a disadvantage of high peak-to-average power ratio (PAPR) [5]. On the other hand, single carrier (SC) transmission has low PAPR. The use of minimum mean square error frequency-domain equalization (MMSE-FDE) can exploit the channel frequency-selectivity to improve the BER performance [6-8].

To limit the signal bandwidth without causing ISI, square-root Nyquist filter can be used as transmit/receive filters [2],[9]. As the filter roll-off factor α increases, the PAPR decreases and furthermore, an additional frequency diversity gain can be obtained by making use of the excess bandwidth introduced by the transmit filtering [10].

However, if the carrier-frequency separation is kept the same as in the case of α=0, the adjacent users' spectra overlap with the desired signal spectrum and the multiuser interference (MUI) is produced, thereby significantly degrading the bit error rate (BER) and throughput performances.

In this paper, we propose two types of frequency-domain iterative MUI cancellation schemes for uplink SC-FDMA using frequency-domain filtering. One is frequency-domain iterative parallel MUI cancellation (FD-IPMUIC) in which joint MMSE-FDE&spectrum combining, and MUI cancellation is carried out for all users in parallel. Another is frequency-domain iterative successive MUI cancellation (FD-ISMUIC). Users are ranked according to their received signal powers. Joint MMSE-FDE&spectrum combining, and MUI cancellation is carried out successively in the descending order of the received signal power.

The remainder of this paper is organized as follows. The SC-FDMA uplink signal transmission using frequency-domain filtering is presented in Sec. II. In Sec. III, we describe the FD-IPMUIC and ISMUIC. In Sec. IV, we evaluate PAPR, BER, and throughput performances by computer simulation. Sec. V concludes this paper.

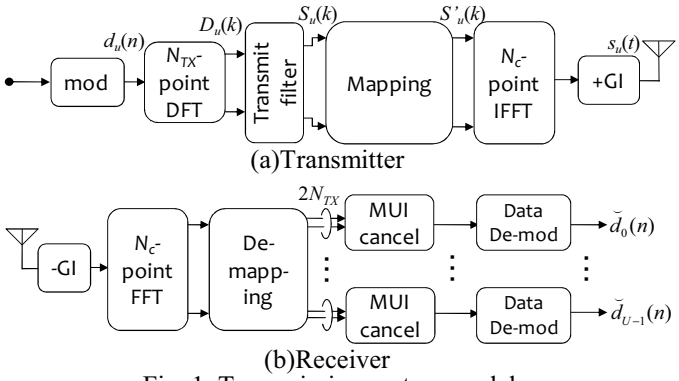

Fig. 1. Transmission system model.

II. SC-FDMA UPLINK SIGNAL TRANSMISSION

The SC-FDMA uplink transmitter/receiver structure is illustrated in Fig. 1. Block transmission of N_{TX} symbols is considered. At the uth(u=0~U–1) user transmitter, the data symbol block $\{d_u(n);n=0\sim N_{TX}-1\}$ is first transformed by N_{TX}-point discrete Fourier transform (DFT) into the frequency-domain signal $\{D_u(k);k=0\sim N_{TX}-1\}$. To limit the signal bandwidth, the square root raised cosine Nyquist filter with the roll-off factor α is applied. The transmit filter transfer function and the filtered frequency-domain signal are denoted by $\{H_T(k);k=-N_{TX}\sim N_{TX}-1\}$ and $\{S_u(k);k=-N_{TX}\sim N_{TX}-1\}$. The frequency-domain signal $\{S_u(k)\}$ after transmit filtering is mapped over N_c subcarriers, where $N_c>>N_{TX}$. In this paper, we consider the localized mapping illustrated in Fig. 2 to prevent the PAPR increases. The carrier-frequency separation is kept the same as in the case of α=0 to accommodate the same number of users. The frequency-domain signal after spectrum mapping is transformed back to the time-domain signal by applying N_c-point inverse FFT (IFFT). Last N_g samples of each block are copied as a cyclic prefix and inserted into the guard interval (GI) placed at the beginning of each block.

The GI-inserted signal block is transmitted over a frequency-selective fading channel. At the receiver, the received signal block $\{r(t);t=0\sim N_c-1\}$ after the removal of the GI, is transformed by applying N_c-point FFT into the frequency-domain signal $\{R(k);k=0\sim N_c-1\}$. Spectrum de-mapping is done to restore each user's spectrum. However, the MUI is produced since adjacent users' spectra overlap with the desired user's spectrum. A series of joint MMSE-FDE&spectrum combining and MUI cancellation are iteratively performed. Finally, the soft

decision variable is obtained by applying N_{TX}-point inverse DFT (IDFT) to the frequency-domain signal after MUI cancelation.

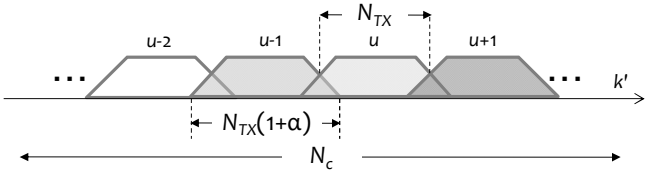

Fig. 2. Spectrum mapping.

A. Transmit Signal

The data symbol block $\{d_u(n);n=0\sim N_{TX}-1\}$ is first transformed by N_{TX}-point discrete Fourier transform (DFT) into the frequency-domain signal $\{D_u(k);k=0\sim N_{TX}-1\}$, to which the transmit filter is applied. The transmit filter output $\{S_u(k);k=-N_{TX}\sim N_{TX}-1\}$ is expressed as

$$S_u(k)=\begin{cases} D_u(k+N_{TX})H_T(k) & k=-N_{TX}\sim -1 \\ D_u(k)H_T(k) & k=0\sim N_{TX}-1 \end{cases}, \quad (1)$$

where

$$D_u(k)=\sqrt{1/N_{TX}}\sum_{n=0}^{N_{TX}-1}d_u(n)\exp\left(-j2\pi kn/N_{TX}\right). \quad (2)$$

The frequency-domain signal $\{S'(k);k=0\sim N_c-1\}$ is obtained after spectrum mapping as shown in Fig. 2. An N_c-point IFFT is applied to $\{S'(k)\}$ to obtain the transmit time-domain signal $s_u(t)$, which is given by

$$s_u(t)=\sqrt{2E_s/T_s}\sqrt{1/N_c}\sum_{k=0}^{N_c-1}S'_u(k)\exp\left(j2\pi kt/N_c\right), \quad t=-N_g\sim N_c-1 \quad (3)$$

where $E_{s,u}$ and T_s denote the symbol energy and symbol duration, respectively.

The propagation channel is assumed to be an L-path block fading channel, each path being subjected to independent fading. Let $h_{u,l}$ and $\tau_{u,l}$ be respectively the complex-valued path gain and delay time of the lth path (l=0~L–1). The channel impulse response is expressed as

$$h_u(\tau)=\sum_{l=0}^{L-1}h_{u,l}\delta(\tau-\tau_{u,l}), \quad (4)$$

where $\delta(\tau)$ is the delta function. The received signal can be expressed as

$$r(t)=\sum_{u=0}^{U-1}\sum_{l=0}^{L-1}h_{u,l}s_u\left(t-\tau_{u,l}\right)+n(t), \quad (5)$$

where $n(t)$ is the zero-mean complex Gaussian noise with variance $2N_0/T_s$ with N_0 being the single-sided power spectrum density of the additive white Gaussian noise (AWGN).

B. Joint MMSE-FDE&Spectrum Combining and MUI cancellation

N_c-point FFT is applied to $\{r(t);t=0\sim N_c-1\}$ to transform it into the frequency-domain signal $\{R(k);k=0\sim N_c-1\}$. $R(k)$ is given by

$$\begin{aligned} R(k)&=\sqrt{1/N_c}\sum_{t=0}^{N_c-1}r(t)\exp(-j2\pi kt/N_c) \\ &=\sum_{u=0}^{U-1}\sqrt{2E_{s,u}/T_s}H'_u(k)S'_u(k)+N(k) \end{aligned}, \quad (6)$$

where $H'_u(k)$ and $N(k)$ are respectively the channel gain and noise due to the AWGN, given by

$$\begin{cases} H'_u(k)=\sum_{l=0}^{L-1}h_{u,l}\exp\left(-j2\pi k\tau_{u,l}/N_c\right) \\ N(k)=\left(\sqrt{1/N_c}\right)\sum_{t=0}^{N_c-1}n(t)\exp\left(-j2\pi kt/N_c\right) \end{cases}. \quad (7)$$

The spectrum de-mapping is applied to $\{R(k)\}$ to obtain the frequency-domain signal $\{R_u(k);k=-N_{TX}\sim N_{TX}-1\}$ and channel gain $\{H_u(k);k=-N_{TX}\sim N_{TX}-1\}$ of the uth user.

The MUI cancellation at the ith iteration stage is explained below. Joint MMSE-FDE&spectrum combing is carried out to obtain the frequency-domain signal $\{\hat{D}_u^{(i)}(k);k=0\sim N_{TX}-1\}$ as

$$\begin{aligned} \hat{D}_u^{(i)}(k)&=\sum_{l=0}^{1}R_u(k-lN_{TX})W_u^{(i)}(k-lN_{TX}) \\ &=\left(\sqrt{2E_{s,u}/T_s}\sum_{l=0}^{1}\hat{H}_u^{(i)}(k-lN_{TX})H_T(k-lN_{TX})\right)D_u(k) \\ &\quad+\sum_{l=0}^{1}M_u(k-lN_{TX})W_u^{(i)}(k-lN_{TX})+\sum_{l=0}^{1}\hat{N}_u^{(i)}(k-lN_{TX}) \end{aligned}, \quad (8)$$

where $\{W_u^{(i)}(k-lN_{TX});l=0,1\}$ is the equalization weight which minimizes the MSE between $D_u(k)$ (the transmitted data block) and $\hat{D}_u^{(i)}(k)$ (the soft decision symbol block). $\hat{H}_u^{(i)}(k)$ and $\hat{N}_u^{(i)}(k)$ are respectively the equivalent cannel gain and noise after FDE, given by

$$\begin{cases} \hat{H}_u^{(i)}(k)=W_u^{(i)}(k)H_u(k) \\ \hat{N}_u^{(i)}(k)=W_u^{(i)}(k)N_u(k) \end{cases}. \quad (9)$$

Then, the cancelation of frequency-domain MUI and residual ISI is carried out as,

$$\breve{D}_u^{(i)}(k)=\hat{D}_u^{(i)}(k)-\tilde{M}_u^{(i)}(k)-\tilde{I}_u^{(i)}(k), \quad (10)$$

where $\tilde{M}_u^{(i)}(k)$ and $\tilde{I}_u^{(i)}(k)$ are respectively the MUI replica and residual ISI replica which will be presented in Sec. III.

Finally, the soft decision symbol block $\{\breve{d}_u^{(i)}(n);n=0,\ldots,N_{TX}-1\}$ is obtained by applying N_{TX}-point IDFT to $\{\breve{D}_u^{(i)}(k):k=0\sim N_{TX}-1\}$ as

$$\breve{d}_u^{(i)}(n)=\sqrt{1/N_{TX}}\sum_{k=0}^{N_{TX}-1}\breve{D}_u^{(i)}(k)\exp\left(-j2\pi kn/N_{TX}\right). \quad (11)$$

C. Frequency-domain Nyquist filtering

In this paper, square root-raised cosine Nyquist filter with roll-off factor α is assumed as the transmit filter whose transfer function $H_T(k)$ is given by

$$H_T(k)=\begin{cases} 1, & 0\le|k|<(1-\alpha)N_{TX}/2 \\ \cos\left[\frac{\pi}{2\alpha}\left(|k|-\frac{1-\alpha}{2N_{TX}}\right)\right], & \frac{1-\alpha}{2}N_{TX}\le|k|<\frac{1+\alpha}{2}N_{TX} \\ 0, & otherwise \end{cases}. \quad (12)$$

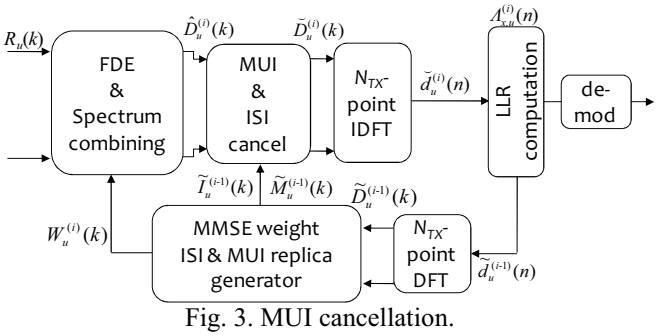

Fig. 3. MUI cancellation.

III. Iterative Interference Cancellation

A. Parallel Interference Cancellation

In this section, we explain how to generate MUI replica and residual ISI replica of the uth users at the ith stage. A series of joint MMSE-FDE&spectrum combining, symbol decision and replica generation is carried out for all users in parallel. The receiver structure for MUI cancellation is illustrated in Fig. 3.

LLR (log-likelihood ratio) of the xth (x=0~m–1) bit in the nth symbols in a block (2^m is the modulation level and n=0~N_{TX}–1) is computed using the decision variable $\{\breve{d}_u^{(i)}(n)\}$ [11] as.

$$\Lambda_{x,u}^{(i-1)}(n)=\ln\left(\frac{p_u^{(i-1)}(b_{n,x}=1)}{p_u^{(i-1)}(b_{n,x}=0)}\right)$$
$$\approx\frac{\left|\breve{d}_u^{(i-1)}(n)-\sqrt{\frac{2E_{s,u}}{T_s}}A_u^{(i-1)}d_{b_{n,x}=0}^{\min}\right|^2}{2\hat{\sigma}_u^{(i-1)^2}}-\frac{\left|\breve{d}_u^{(i-1)}(n)-\sqrt{\frac{2E_{s,u}}{T_s}}A_u^{(i-1)}d_{b_{n,x}=1}^{\min}\right|^2}{2\hat{\sigma}_u^{(i-1)^2}} \quad ,(13)$$

where $p_u^{(i-1)}(b_{n,x}=0)$ and $p_u^{(i-1)}(b_{n,x}=1)$ are the probabilities of the transmitted bit $b_{n,x}$ being $b_{n,x}$=0 and $b_{n,x}$=1, respectively, when expected at the (i–1)th iteration stage. $d_{b_{n,x}=0}^{\min}$ (or $d_{b_{n,x}=1}^{\min}$) is the symbol whose xth bit is 0 (or 1) and has the shortest Euclidean distance from $\hat{d}_u^{(i-1)}(n)$. $2\hat{\sigma}_u^{(i-1)^2}$ is the variance of MUI, residual ISI plus noise and is given by,

$$\begin{aligned}2\hat{\sigma}_u^{(i)^2}&=2\hat{\sigma}_{u,MUI}^{(i)^2}+2\hat{\sigma}_{u,ISI}^{(i)^2}+2\hat{\sigma}_{u,noise}^{(i)^2}\\&=2\frac{E_{s,u-1}}{T_s}\rho_{u-1}^{(i-1)}\left(\frac{1}{N_{TX}}\sum_{k=-N_{TX}}^{N_{TX}-1}\left|H_{u-1}(k)H_T(k)W_u^{(i)}(k-N_{TX})\right|^2\right)\\&+2\frac{E_{s,u+1}}{T_s}\rho_{u+1}^{(i-1)}\left(\frac{1}{N_{TX}}\sum_{k=-N_{TX}}^{N_{TX}-1}\left|H_{u+1}(k)H_T(k)W_u^{(i)}(k+N_{TX})\right|^2\right),\\&+2\frac{E_{s,u}}{T_s}\rho_u^{(i-1)}\left(\frac{1}{N_{TX}}\sum_{k=-N_{TX}}^{N_{TX}-1}\left|\hat{H}_u^{(i)}(k)H_T(k)\right|^2-\left|A_u^{(i)}\right|^2\right)\\&+2\frac{N_0}{T_s}\frac{1}{N_{TX}}\sum_{k=-N_{TX}}^{N_{TX}-1}\left|W_u^{(i)}(k)\right|^2\end{aligned} \quad (14)$$

where

$$A_u^{(i)}=(1/N_{TX})\sum_{k=-N_{TX}}^{N_{TX}-1}\hat{H}_u^{(i)}(k)H_T(k). \quad (15)$$

Assuming QPSK data modulation, the soft symbol replica $\{\tilde{d}_u^{(i)}(n)\}$ is given as [11]

$$\tilde{d}_u^{(i-1)}(n)=\frac{1}{\sqrt{2}}\tanh\left(\frac{\Lambda_{0,u}^{(i-1)}(n)}{2}\right)+j\frac{1}{\sqrt{2}}\tanh\left(\frac{\Lambda_{1,u}^{(i-1)}(n)}{2}\right) \quad (16)$$

The symbol replica block $\{\tilde{d}_u^{(i)}(n)\}$ is transformed into the frequency domain signal $\{\tilde{D}_u^{(i-1)}(k);k=0\sim N_{TX}-1\}$ by applying N_{TX}-point DFT as

$$\tilde{D}_u^{(i-1)}(k)=\left(\sqrt{1/N_{TX}}\right)\sum_{n=0}^{N_{TX}-1}\tilde{d}_u^{(i-1)}(n)\exp\left(-j2\pi kn/N_{TX}\right), \quad (17)$$

where $\tilde{d}_u^{(-1)}(n)=0$. The frequency-domain MUI replica $\tilde{M}_u^{(i)}(k)$ and residual ISI replica $\tilde{I}_u^{(i)}(k)$ are generated using $\tilde{D}_{u-1}^{(i-1)}(k)$, $\tilde{D}_{u+1}^{(i-1)}(k)$ (adjacent users' spectra overlap with the desired uth user's spectrum) and $\tilde{D}_u^{(i-1)}(k)$ as

$$\begin{aligned}\tilde{M}_u^{(i)}(k)&=\sqrt{\frac{2E_{s,u-1}}{N_0}}\left(\sum_{l=0}^{1}\frac{H_{u-1}(k-lN_{TX})H_T(k-lN_{TX})}{W_u^{(i)}(k-(l+1)N_{TX})}\right)\tilde{D}_{u-1}^{(i-1)}\\&+\sqrt{\frac{2E_{s,u+1}}{N_0}}\left(\sum_{l=0}^{1}\frac{H_{u+1}(k-lN_{TX})H_T(k-lN_{TX})}{W_u^{(i)}(k-(l-1)N_{TX})}\right)\tilde{D}_{u+1}^{(i-1)}\end{aligned} \quad (18)$$

$$\tilde{I}_u^{(i)}(k)=\sqrt{\frac{2E_{s,u}}{N_0}}\left(\sum_{l=0}^{1}\hat{H}_u^{(i)}(k-lN_{TX})H_T(k-lN_{TX})-A_u^{(i)}\right)\tilde{D}_u^{(i-1)} \quad (19)$$

for FD-IPMUIC. MUI cancellation is carried out according to Eq. (10).

B. Succesive Interference Cancellation

In FD-ISMUIC, users are ranked according to their received signal powers. A series of joint MMSE-FDE&spectrum combining, symbol decision and replica generation is carried out in de descending order of the received signal power. The uth users' received signal power P_u is given by

$$P_u=(1/N_{TX})\sum_{k=-N_{TX}}^{N_{TX}-1}\left|H_u(k)H_T(k)\right|^2. \quad (20)$$

$\{P_u;u=0\sim U-1\}$ are compared and users are ranked in the descending order. In this paper, we assume $P_0\geq P_1\geq\ldots\geq P_u\geq\ldots\geq P_{U-1}$ without loss of generality. The replica generation is almost the same as for FD-IPMUIC. The difference from FD-IPMUIC is that the signal detection is done in the descending order of the received signal power. The frequency-domain MUI replica $\{\tilde{M}_u^{(i)}(k)\}$ for uth user is generated using $\tilde{D}_{u-1}^{(i)}(k)$ and $\tilde{D}_{u+1}^{(i-1)}(k)$ (the (u+1)th user has not been detected yet in the current iteration stage and therefore, the frequency-domain signal regenerated at the previous iteration stage is used) as

$$\begin{aligned}\tilde{M}_u^{(i)}(k)&=\sqrt{\frac{2E_{s,u-1}}{N_0}}\left(\sum_{l=0}^{1}\frac{H_{u-1}(k-lN_{TX})H_T(k-lN_{TX})}{W_u^{(i)}(k-(l+1)N_{TX})}\right)\tilde{D}_{u-1}^{(i)}\\&+\sqrt{\frac{2E_{s,u+1}}{N_0}}\left(\sum_{l=0}^{1}\frac{H_{u+1}(k-lN_{TX})H_T(k-lN_{TX})}{W_u^{(i)}(k-(l-1)N_{TX})}\right)\tilde{D}_{u+1}^{(i-1)}\end{aligned} \quad .(21)$$

MUI cancellation is carried out according to Eq. (10).

For FD-ISMUIC, the variance of MUI in Eq. (14) is given by,

$$\begin{aligned}&2\hat{\sigma}_{u,MUI}^{(i)^2}\\&=2\frac{E_{s,u-1}}{T_s}\rho_{u-1}^{(i)}\left(\frac{1}{N_{TX}}\sum_{k=-N_{TX}}^{N_{TX}-1}\left|H_{u-1}(k)H_T(k)W_u^{(i)}(k-N_{TX})\right|^2\right)\\&+2\frac{E_{s,u+1}}{T_s}\rho_{u+1}^{(i-1)}\left(\frac{1}{N_{TX}}\sum_{k=-N_{TX}}^{N_{TX}-1}\left|H_{u+1}(k)H_T(k)W_u^{(i)}(k+N_{TX})\right|^2\right)\end{aligned} \quad .(22)$$

C. Adaptive MMSE-FDE Weights

In this section, we derive MMSE-FDE weights of FD-IPMUIC and FD-ISMUIC. The MMSE-FDE weight minimizes the MSE between the frequency-domain signal after interference cancellation, $\{\tilde{D}_u^{(i)}(k);k=0\sim N_{TX}-1\}$, and that of the transmitted data symbol block, $\{D_u(k);k=0\sim N_{TX}-1\}$. The MMSE-FDE weight $W_u^{(i)}(k)$ at the ith stage for the uth user is given by

$$W_u^{(i)}(k)=\frac{H_u^*(k)H_T^*(k)}{\left(\begin{array}{l}\rho_u^{(i-1)}\sum_{l=0}^{1}\left|H_u(k-lN_{TX})H_T(k-lN_{TX})\right|^2\\+\rho_{u-1}^{(i-1)}\left|H_{u-1}(k+N_{TX})H_T(k+N_{TX})\right|^2\\+\rho_{u+1}^{(i-1)}\left|H_{u+1}(k-N_{TX})H_T(k-N_{TX})\right|^2+(E_s/N_0)^{-1}\end{array}\right)}, \quad (23)$$

for FD-IPMUIC and

$$W_u^{(i)}(k)=\frac{H_u^*(k)H_T^*(k)}{\left(\begin{array}{l}\rho_u^{(i-1)}\sum_{l=0}^{1}\left|H_u(k-lN_{TX})H_T(k-lN_{TX})\right|^2\\+\rho_{u-1}^{(i)}\left|H_{u-1}(k+N_{TX})H_T(k+N_{TX})\right|^2\\+\rho_{u+1}^{(i-1)}\left|H_{u+1}(k-N_{TX})H_T(k-N_{TX})\right|^2+(E_s/N_0)^{-1}\end{array}\right)}, \tag{24}$$

for FD-ISMUIC, where $\rho_u^{(i)}$ is given as [11]

$$\begin{aligned}\rho_u^{(i)}&=E[|D_u(k)-\tilde{D}_u^{(i)}(k)|^2]\\&=(1/N_{TX})\sum_{n=0}^{N_{TX}-1}\left(E[|d_u(n)|^2]-|\tilde{d}_u^{(i)}(k)|^2\right).\end{aligned} \tag{25}$$

In the above, $E[|d_u(n)|^2]$ of Eq. (25) is the expectation of the transmitted symbol block using the *a posteriori* probability of the transmitted block for the given received signal block $\{r(t);t=0\sim N_c-1\}$ (note that for QSPK data modulation, $E[|d_u(n)|^2]=1$ always). It can be understood from Eqs. (23) and (24) that the MMSE-FDE weight acts as the matched filter to the transmit filter (the numerator includes the complex conjugate of the transmit filter transfer function $H_T(k)$).

IV. Computer Simulation

The simulation condition is summarized in Table 1. A block transmission of N_{TX}=64 and QPSK data modulation is assumed. We assume an L=16-path frequency-selective block Rayleigh fading channel having uniform power delay profile (i.e., $E[|h_{u,l}|^2]=1/L$ for all l). The transmit timing is asynchronous among different users, but is assumed to be kept within the GI. Ideal channel estimation and ideal slow transmit power control ($E_{s,u}=E_s$ for all user) are also assumed.

Table. 1 Simulation condition

Transmitter	Data modulation	QPSK
	Number of symbols per block	N_{TX}=64
	FFT/IFFT block size	N_c=256
	GI length	N_g=32
Transmit/receive filters	Transfer function	Square-root raised cosine
	Roll off factor	α=0~1
Channel	Fading type	Frequency-selective block Rayleigh
	Power delay profile	L=16-path uniform power delay profile
	Time delay	$\tau_{u,l}=l$, l=0~L-1
Receiver	Interference cancellation	FD-IPMUIC,ISMUIC
	Channel estimation	Ideal

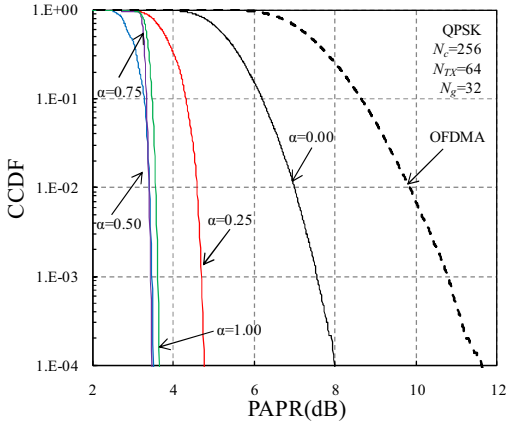

Fig.4 CCDF of PAPR.

A. PAPR

PAPR is defined as [12]

$$\text{PAPR}=\frac{\max\{|s_u(t)|\}_{t=0\sim N_c-1}}{E[|s_u(t)|^2]}. \tag{26}$$

The complementary cumulative distribution function (CCDF) of the PAPR is plotted in Fig. 4 with the roll-off factor α as a parameter. As α increases, the $\text{PAPR}_{0.1\%}$ level, which the PAPR exceeds with a probability of 0.1%, decreases, but it becomes almost the same beyond α=0.5. When α=0.5, the PAPR level can be reduced by 4.1dB at the cost of increased bandwidth, compared to the case of α=0. How much performance improvement is obtained by the bandwidth increase will be discussed in the following subsections.

B. BER performance

The impact of the number i of iterations on BER is plotted for FD-IPMUIC and FD-ISMUIC in Fig. 5 when the average received bit energy-to-noise power spectrum density ratio E_b/N_0=12 dB, where E_b/N_0 given by $(1/m)(1+N_g/N_c)(E_s/N_0)$ with m being the number of bits per symbol. For comparison, the BER is also plotted for the single-user case (note that iterative ISIC [11] is used). When i=0, the BER is more than 10^{-2} due to a severe MUI. However, as i increases, the BER reduces. When i=5, PMUIC and SMUIC can sufficiently suppress MUI and the BER close to single-user case can be achieved. Therefore, i=5 is assumed below.

The BER performance is plotted for FD-IPMUIC and FD-ISMUIC in Fig. 6 as a function of E_b/N_0. For comparison, the BER performance is also plotted for the single-user case (note that iterative ISIC [11] is used). It can be seen from Fig. 6 that FD-ISMUIC is superior to FD-IPMUIC since ISMUIC users the detection order based on the received signal power and can generate more accurate MUI replicas.

C. Throughput performance

Packet error rate (PER) was measured assuming FD-ISMUIC with i=5. Each packet consists of two blocks (1024 bits). The throughput η(bps/Hz) is computed using [14]

$$\eta=2\times(1-\text{PER})\times(1+N_g/N_c)^{-1}. \tag{27}$$

The throughput performance is plotted as a function of the average received E_s/N_0 in Fig. 7. It can be seen from Fig. 7 that the throughput improves as α increases. This is because FD-ISMUIC can sufficiently suppress the MUI and ISI and because as α increases, an additional frequency diversity gain can be obtained.

The peak E_s/N_0 is an important design parameter which determines the required peak transmit power of terminal transmitter power amplifiers. The throughput performance is plotted as a function of peak E_s/N_0 in Fig. 8. In this paper, peak E_s/N_0 is defined as peak E_s/N_0=average received E_s/N_0 + $\text{PAPR}_{0.1\%}$ [13]. It can be seen from Fig. 8 that the throughput improvement is more pronounced due to the reduced PAPR.

V. Conclusion

In this paper, we proposed two types of frequency-domain iterative MUI cancellation schemes, FD-IPMUIC and FD-ISMUIC, for uplink SC-FDMA using frequency-domain filtering. Both schemes can achieve the frequency diversity gain through joint MMSE-FDE&spectrum combing. In FD-ISMUIC the interference cancellation is done successively according to the user ranking based on the received signal power measurement and therefore, better performance can be achieved than FD-IPMUIC. The PAPR, BER and throughput performance with the proposed scheme were evaluated by computer simulation to show that the proposed schemes can

achieve the BER performance close to the single user case. As the filter roll-off factor α increases, the throughput performance improves since larger frequency diversity gain is obtained. The throughput improvement is more pronounced when the throughput performance vs. peak E_s/N_0 is considered.

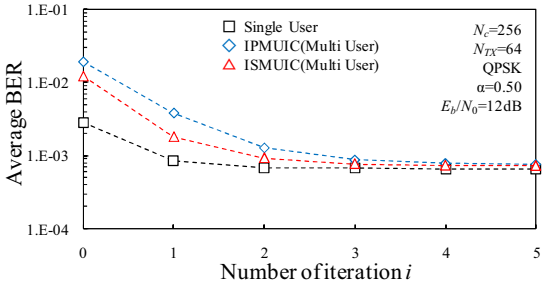

(a) α=0.5

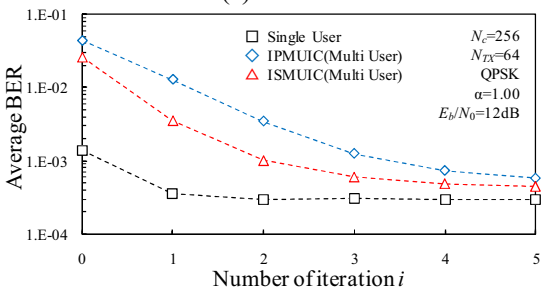

(b) α=1

Fig.5 Impact of the number of iterations, i.

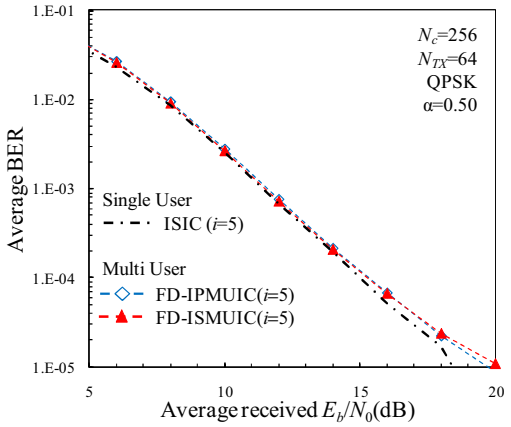

(a) α=0.5

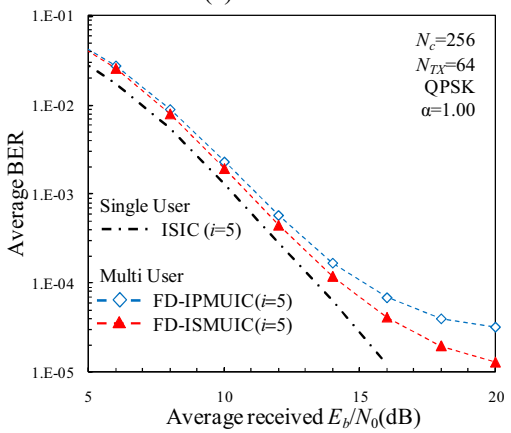

(b) α=1

Fig.6 BER performance.

REFERENCES

[1] W. C., Jakes Ir., Ed,. *Microwave mobile communications*, Wiley, New York, 1974.

[2] J. G Proakis, Digital communications, 4th ed., McGraw-Hill, 2001.

[3] R. Prasad, *OFDM for wireless communications systems*, Artech House, 2004.

[4] S. Hara and R. Prasad, *Multicarrier techniques for 4G mobile communications*, Artech House, 2003.

[5] J. Armstrong, "New OFDM peak-to-average power reduction scheme," Proc. IEEE 54th Veh. Technol. Conf. (VTC), Vol. 1, pp. 756-760, Oct. 2001.

[6] D. Falconer, S. L. Ariyavisitakul, A. Benyamin-Seeyarand B. Edison, "Frequency domain equalization for single-carrier broadband wireless systems," IEEE Commun. Mag., Vol.40, No. 4, pp.58-66. Apr. 2002.

[7] F. Adachi, D. Garg, S. Takaoka, and K. Takeda, "Broadband CDMA techniques," IEEE Wireless Commun., Mag., Vol. 12, No. 2, pp. 8-18, Apr. 2005.

[8] F. Adachi and K. Takeda, "Bit error rate analysis of DS-CDMA with joint frequency-domain equalization and antenna diversity reception," IEICE Trans. Commun., Vol. E87-B, No. 10, pp. 2991-3002, Oct. 2004.

[9] Y. Akaiwa, *Introduction to digital mobile communication*, Wiley, New York, 1997.

[10] S. Okuyama, K, Takeda and F, Adachi, "MMSE frequency-domain equalization using spectrum combining for Nyquist filtered broadband single-carrier transmission," to be presented at The 71th Veh. Technol. Conf. (VTC2010-spring), May 2010.

[11] K. Takeda, K. Ishihara and F. Adachi, "Frequency-Domain ICI Cancellation with MMSE Equalization for DS-CDMA Downlink," IEICE Trans. Commun., Vol.E89-B No.12, pp.3335-3343, Dec. 2006.

[12] H. G. Myung, J. Lim, and D. J. Goodman, "Single Carrier FDMA for Uplink Wireless Transmission", *IEEE Vehicular Technology Magazine*, vol. 3, no. 1, Sep. 2006, pp. 30-38.

[13] H. Gacanin and F. Adachi, "A Comprehensive Performance Comparison of OFDM/TDM Using MMSE-FDE and Conventional OFDM," Proc. IEEE 67th Veh. Technol. Conf. (VTC), pp.11-14, May, 2008.

[14] K. Fukuda, A. Nakajima, and F. Adachi, "LDPC-coded HARQ Throughput Performance of MC-CDMA using ICI Cancellation," Proc. IEEE 66th Veh. Technol. Conf. (VTC), pp.965-969, Sept., 2007.

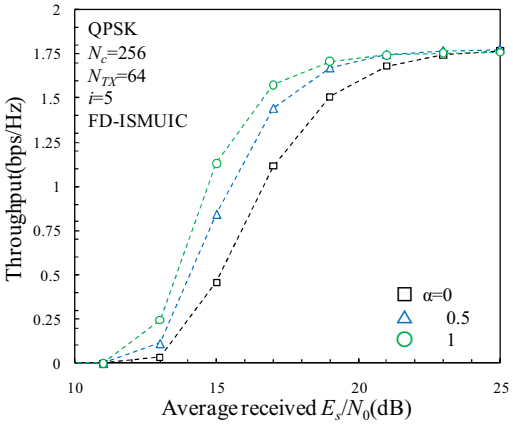

Fig. 7 Throughput vs. average received E_s/N_0.

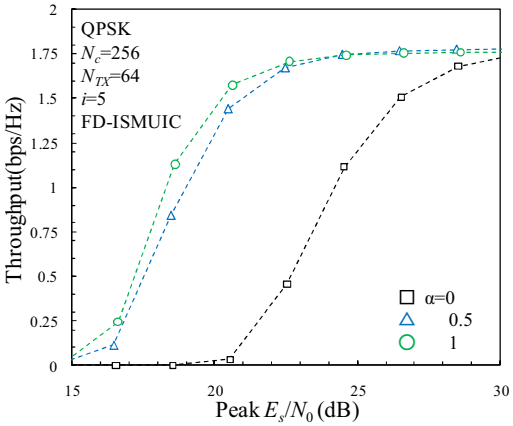

Fig.8 Throughput vs. peak E_s/N_0